International Journal Of Scientific And University Research Publication

ISSN No 311/714

Listed & Index with
ISSN Directory. Paris

Multi-Subject Journal

Volum : (16) | Issue : 210 |

INTERNATIONAL JOURNAL OF SCIENTIFIC AND UNIVERSITY RESEARCH PUBLICATION

Research Paper

MORE BULLETS FOR PISTOL: LINEAR AND CYCLIC SILOXANE REPORTER PROBES FOR QUANTITATIVE 1H MR OXIMETRY

Shubhangi Agarwal || These authors contributed equally.

ملخص

Tissue oximetry can assist in diagnosis and prognosis of many diseases and enable personalized therapies. Previously, we reported the ability of hexamethyldisiloxane (HUDSON) for accurate measurements of tissue oxygen tension (PO_2) using Proton Imaging of Siloxanes to map Tissue Oxygenation Levels (PISTOL) magnetic resonance imaging. Here we report the feasibility of several commercially available linear and cyclic siloxanes (molecular weight 162–410 g/mol) as PISTOL-based oxygen reporters by characterizing their calibration constants. Further, field and temperature dependence of PO_2 calibration curves of HMDSO, octamethyltrisiloxane (OMTSO) and polydimethylsiloxane (PDMSO) were also studied. The spin-lattice relaxation rate R_1 of all siloxanes studied here exhibited a linear relationship with oxygenation ($R_1 = A' + B'*PO_2$) at all temperatures and field strengths evaluated here. The sensitivity index η(= B′/A′) decreased with increasing molecular weight with values ranged from 4.7×10^{-3}–11.6×10^{-3} $torr^{-1}$ at 4.7 T. No substantial change in the anoxic relaxation rate and a slight decrease in PO_2 sensitivity was observed at higher magnetic fields of 7 T and 9.4 T for HMDSO and OMTSO. Temperature dependence of calibration curves for HMDSO, OMTSO and PDMSO was small and simulated errors in pO_2 measurement were 1–2 torr/°C. In summary, we have demonstrated the feasibility of various linear and cyclic siloxanes as PO_2-reporters for PISTOL-based oximetry.

الكلمات الرئيسية

This work was supported by NIH 1R21CA132096-01A1, a National Science

regarding oxygenation. The current magnetic resonance imaging (MRI) based oximetry techniques can be further sub-divided into a) , [32]qualitative techniques: Blood Oxygen Level Dependent (BOLD) , [34], oxygen-enhanced MRI[33]Tissue Oxygen Level Dependent (TOLD) and b) quantitative oximetry techniques: [35]hypoxia targeted MRI F NMR of [19]), [36]Electron Paramagnetic Resonance (EPR perfluorocarbon emulsions, Fluorocarbon Relaxometry using F [19]Echoplanar imaging for Dynamic Oxygen Mapping (FREDOM, and Proton Imaging of Siloxanes for [37]MRI of hexafluorobenzene)).[38,39]mapping Tissue Oxygenation Levels (PISTOL)

H) techniques are minimally [1]F and [19]EPR and MR oximetry (invasive and provide quantitative oxygenation information via measuring the change in linewidth or spin lattice relaxation time, respectively, of an exogenously administered paramagnetic spin -probe as it interacts with the molecular oxygen. They allow for non invasive and repeated measurement of oxygenation at multiple locations. Some of the EPR probes are lithium phthalocyanine (LiPc), lithium naphthalocyanine (LiNc), Fusinite, Gloxy, India Ink and triarylmethyl (TAM), of which India Ink is approved for clinical F MR oximetry uses exogenous perfluorocarbon [19]. The [36,40]use) or [41]reporters such as perfluoro-15-crown-5-ether (15C5 as oxygen reporters and uses the linear [37,42,43]hexafluorobenzene with [1]relationship of flurocarbon spin-lattice relaxation rate R oxygenation. Exploiting the same concept, our group has previously shown the feasibility of accurate and repeated measurements of oxygen using hexamethyldisiloxane (HMDSO) in thigh muscle and . We have also shown[38,39]H MR oximetry[1] using *in vivo*tumor regions as [44]the ability of siloxane based nanoemulsions for tissue oximetry . Siloxanes can be synthesized in a [45,46]well as cellular oximetry variety of forms (linear or cyclic, increasing chain length, with or without functional groups) and have been used in various applications . While [47]such as biomedicine, cosmetics, and food processing reporter and has a large [2]HMDSO has been shown to be a reliable PO , the values of spin lattice [38] sensitivity[2]dynamic range and high pO) under hypoxic conditions can be as long [1] (= $1/R_1$relaxation time T as 11 s, leading to long measurement times. This raises the question reporter [2]whether any of the other siloxanes could be used as PO molecules and how chain length and structure (linear versus cyclic) exhibited [1] sensitivity and dynamic range of T_2influence the PO under different oxygenation conditions. In this study, we have characterized the calibration curves of various low molecular weight sensing [2]linear and cyclic siloxanes and assessed their utility as pO H MR oximetry. The siloxanes [1]reporter molecules for use with investigated here are: linear siloxanes HMDSO, octamethyltrisiloxane

مقدمة

Adequate availability of oxygen is critical to the efficient functioning . Changes in oxygenation are [1]of many vital organs and tissues indicative of a disruption in homeostatic conditions which are , ischemic heart [3,4], wounds[2]prevalent in pathologies such as tumors . The [10] and traumatic brain injury[7,8,9] metabolic disorders[5,6]disease oxygen requirement changes between cells, tissues and organs and thus each tissue type exhibits a distinct normal range of oxygenation. For example, the normal tissue oxygen level in the brain is ~34 torr . The lack of adequate [11](mmHg) while that in the muscle is ~29 torr oxygen in cells and tissues is termed as hypoxia and could result from diminished blood flow, low blood oxygen saturation, elevated oxygen metabolism and increased cellular proliferation. Oxygen homeostasis and hypoxic stress are being recognized as important factors for development and physiology of cells and tissues. These factors also influence the pathophysiology of diseases as they regulate various intracellular signaling pathways for processes such as angiogenesis, . Malignant [12,13,14,15,16,17,18]cell proliferation and protein synthesis tumors are known to have regions with low oxygen tension known as hypoxia which is a major driving force behind tumor progression and . Hypoxia presents itself as an ideal target[19,20,21]resistance to therapies for the development of anti-cancer therapies due to the role that it . Thus, measurement of oxygen is [22]plays in the progression of cancer essential for monitoring the function of organs as well as for diagnosis, treatment planning and studying treatment response of pathologies. Consequently, there is an increased need for an oximetry technique that can facilitate repeated, non-invasive and accurate assessment of oxygen and can be translated to the clinic.

Many qualitative and quantitative oximetry techniques have been , [23]developed for oximetry such as polarographic needle electrode , [24], Near Infrared (NIR) spectroscopy[23]fiber optic probes , positron emission [26], immunohistochemical probes[25]fluorescence and single photon emission computed [27]tomography (PET) . Polarographic needle electrode and fiber [28]tomography (SPECT) optic probe techniques are invasive, susceptible to pressure artifacts and cannot facilitate simultaneous measurement of multiple locations and repeated measurements, while immunohistochemical hypoxia) are limited[26], HIF1α[30], EF5[29]probes (pimonidazole analysis. NIR spectroscopy is a non-invasive technique but *ex-vivo*to can only detect the changes in vascular oxygen saturation and cannot distinguish between signals from oxyhemoglobin, deoxyhemoglobin, . PET and SPECT based techniques lack [31] oxidase*c*and cytochrome spatial resolution and cannot provide quantitative information

k is a constant that determines the solubility of oxygen in the agent and is different for different agents. Thus, net relaxation rate becomes

$$1=A′+B′∗pO2R1=A′+B′∗pO2$$

(3)

/k_{1p} and B′ = $R_{1d}$where A′ = R

Since longitudinal relaxation rate is a function of temperature we assume a linear dependence of constants A′ and B′ on temperature (for relevant physiological range) which empirically can be defined as

$$A′=A+C∗TA′=A+C∗T$$

(4)

$$B′=B+D∗TB′=B+D∗T$$

(5)

-Substituting value of A′ and B′ in Eq. [3] results in a temperature dependent model for net relaxation rate

$$1=A+B∗pO2+C∗T+D∗T∗pO2$$
$$R1=A+B∗pO2+C∗T+D∗T∗pO2$$

(6)

levels can be $_2$Inverting the above equation, quantitative pO determined more accurately and reliably if temperature is also monitored.

$$p$$

(OMTSO), decamethyltetrasiloxane (DMTSO), dodecamethylpentasiloxane (DDMPSO), trimethylsiloxy-terminated polydimethylsiloxane (PDMSO, M.W. 410) and cyclic siloxanes octamethylcyclotetrasiloxane (OMCTSO) and decamethylcyclopentasiloxane (DMCPSO). These siloxanes are H resonance [1]commercially available, inexpensive and have a single . Further, field and temperature dependence of the [48]around 0.1 ppm calibration curves of HMDSO, OMTSO and PDMSO were also $_2$PO studied.

Theory

Quantitative MR oximetry exploits the Fermi contact interactions that leads to a [49]between paramagnetic oxygen and reporter molecules) dependent relaxation of the nuclear$_2$ concentration (and hence pO_2O MR oximetry must preferably possess *in vivo*spins. Probes used for the following characteristics: high oxygen solubility, hydrophobicity (so that diffusion of aqueous ions is restricted), should have a single resonance so that there are no chemical shift artifacts in the MR on temperatures. Due to $_1$images and minimal dependence of R paramagnetic nature of molecular oxygen, it tends to shorten the nuclear relaxation times and relaxes the nuclear spins faster thereby increasing the spin-lattice (longitudinal) and spin-spin (transverse) respectively of the reporter molecule. The $_2$ and R_1relaxation rate R on the spin-lattice $_2$principle is based on the linear dependence of pO relaxation rate of the probe.

If x is the molar fraction of oxygen the net spin lattice relaxation rate [49] is given by$_1$R

$$1=(1−x)∗R1d+x∗(R1d+R1p)=R1d+x∗R1p$$

$$R1=(1−x)∗R1d+x∗(R1d+R1p)=R1d+x∗R1p$$

$$R$$

(1)

= diamagnetic or anoxic component of the relaxation rate $_{1d}$Where R and

= paramagnetic component of the relaxation rate due to the $_{1p}$R contribution of oxygen.

is directly related to *x*As per Henry's law, the dissolved mole fraction the partial pressure of oxygen.

$$pO2=k∗xpO2=k∗x$$

(2)

Relative Signal $(\alpha)^{siloxane}$	η (X10^{-3}) = B′/A′	Slope B′ (s*torr)$^{-1}$	Intercept A′ (s^{-1})	Molecular wt. (g/mol)	Siloxane
1.00	11.6	0.0013 ± 2.09 × 10^{-5}	0.1125 ± 1.38 × 10^{-3}	162.4	HMDSO*
0.98	11.4	0.0012 ± 8.38 × 10^{-5}	0.1597 ± 7.50 × 10^{-3}	236.5	OMTSO
0.97	8.4	0.0015 ± 3.60 × 10^{-5}	0.1780 ± 3.30 × 10^{-3}	310.7	DMTSO
0.97	8.2	0.0017 ± 7.44 × 10^{-5}	0.2062 ± 6.70 × 10^{-3}	384.8	DDMPSO
0.91	5.6	0.0016 ± 3.87 × 10^{-5}	0.2827 ± 3.50 × 10^{-3}	296.6	OMCTSO
0.92	4.7	0.0015 ± 3.47 × 10^{-5}	0.3169 ± 3.10 × 10^{-3}	370.8	DMCPSO

Table 1 Summary of calibration constants and α of the ^{siloxane} various linear and cyclic siloxanes at 4.7 T (37 °C).

Results

Calibration curves of linear and cyclic siloxanes at 4.7 T

of the linear and cyclic siloxanes (Fig. 1) OMTSO, DMTSO, $_1$R DDMPSO, OMCTSO and DMCPSO were measured as a function of at 4.7 T and 37 °C and fit to the Eq. [3] to yield the calibration $_2$pO of all the $_1$constants A′ and B′. At a fixed temperature (37 °C), the R > 0.99) (Fig. 2). In ^{2} (R$_2$siloxanes showed a linear dependence on pO the linear siloxanes, it was observed that with increasing molecular weight, the intercepts of the linear fits increased (ranging from) but the slopes were almost similar (ranging from 1.3 × $^{-1}$0.11–0.32 s). The cyclic compounds had higher $^{-1}$.torr^{-1}s $^{-3}$ −1.7 × 10^{-3}10 than the linear compounds at each oxygen concentration and $_1$R showed a similar trend with increasing molecular weight as the linear siloxanes. The recovery curves for all siloxanes showed a monoexponential behavior (Supplementary Fig. S1). Table 1 lists the values of the calibration constants A′ and B′ for all the linear and values. ^{siloxane}cyclic siloxanes at 4.7 T and 37 °C along with the α HMDSO calibration constants at 4.7 T were included from our for comparison.[38] previously published work

Figure 1

$$2=O$$

$$C*TB+D*TpO2=R1-A-C*TB+D*T$$

(7)

Therefore, estimation of these parameters (A, B, C and D) is crucial measurement. Equation [7] also allows us to relate $_2$for accurate pO estimation at a particular oxygenation level and $_2$the errors in pO temperature to the potential errors or uncertainty in temperature applications. Also, for a given *in vivo*measurement, particularly for determination per 1 °C $_2$ measurement, the relative error in pO$_1$R error in temperature estimation at a particular temperature T and can be derived as:$_2$oxygenation level pO

$$pO2\Delta T=|C+D*pO2||B+D*T|$$

$$\Delta pO2\Delta T=|C+D*pO2||B+D*T|$$

(8)

While comparing signals from same volumes of various siloxanes (as), the*in vivo*typically a fixed volume of reporter probe would be used , of each (compared to HMDSO) ^{siloxane}relative theoretical signals, α can be computed by accounting for the density differences and the mole fraction of protons in a mole of the siloxane.

$$siloxane=\rho siloxane*NsiloxaneH*MWH$$

$$MDSO\rho HMDSO*NHMDSOH*MWsilox$$

$$ane.$$

$$\propto siloxane=\rho siloxane*NHsiloxane*MWHM$$

$$DSO\rho HMDSO*NHHMDSO*MWsiloxane$$

(9)

$$\rho silo$$

Where,

$$xane\rho siloxane$$

is the density of the siloxane under

$$Nsiloxane HNH siloxane$$

is the number of H atoms (5.764 g/ml for HMDSO at 25 °C),

$$MWsiloxane MWsiloxane$$

is the molecular weight of the siloxane (162 g/mol for HMDSO). The theoretical values of are listedin Table 1. $^{siloxane}\alpha$

VOL- (16) ISSUE 210 ISSN 311/714

Temperature and field dependence of calibration of siloxanes

was determined at 7 T $_2$ of HMDSO on PO_1The dependence of R (Fig. 3A,B) and 9.4 T (Fig. 3C,D) as a function of temperature and was observed to be linear at both fields at all temperatures measured. Constants A′ and B′ were then plotted with respect to variations in temperature, in the physiologically relevant range of 17 °C to 48 °C, to yield characterization parameters A, B, C and D (Eqs. [4] and [5]) at 7 T (Supplementary Fig. S2A,B) and 9.4 T (Supplementary error (Eq. [8]) $_2$Fig. S2C,D). These are listed in Table 2. Relative PO was computed based on these constants and was found to be between range 0–50 torr at 7 $_2$0.6–1 torr/°C in the physiologically relevant pO error was ~ $_2$T (Supplementary Fig. S2E). In contrast, the relative pO 1 torr/°C at 9.4 T showing very small variation between 0–50 torr of 5 torr, resulting error in $_2$(Supplementary Fig. S2E). E.g. for a PO determination per degree change in temperature at 37 °C was ~ $_2$PO 0.7 torr/°C at 7 T and ~ 1 torr/°C at 9.4 T.

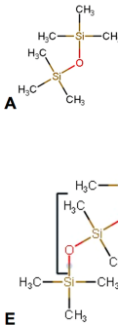

Figure 3 2D structures of the various linear and cyclic siloxanes characterized) hexamethyldisiloxane (HMDSO), **A**in this study. Linear siloxanes: ( ) decamethyltetrasiloxane **C**) octamethyltrisiloxane (OMTSO), (**B**( ) **E**) dodecamethylpentasiloxane (DDMPSO), (**D**(DMTSO), (((O).

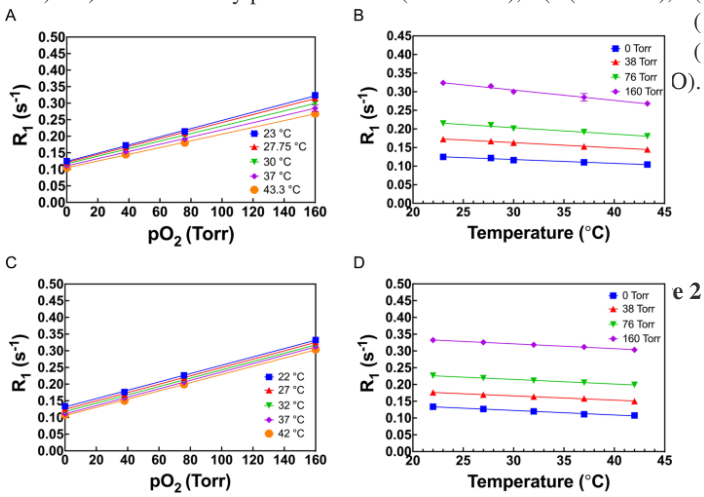

e 2

of HMDSO at 7 T $_1$Dependence of spin lattice relaxation rate R).**D**,**B**) and temperature (**C**,**A** ($_2$) on pO**C**,**D**) and 9.4 T(**B**,**A**(

η ( ) $^{-3}$X10 = B′/A′	Slope B′	Interce pt)$^{-1}$A′ (s 37 °C	D (s*to r $^{-1}$r*°C)	C ($^{-1}$s*°C)	B $^{-1}$	)$^{-1}$A (s	Field	Siloxan e
	37 °C	$^{-1}$						

(at 37 °C and $_2$ on PO_1Dependence of spin lattice relaxation rate R 4.7 T) for linear and cyclic siloxanes of different chain lengths. The cyclic compounds displayed higher longitudinal relaxation rates than the linear compounds at all oxygen concentrations. *Data from , 743–748) reproduced**55**., Magn Reson Med *et al*ref 38 (Kodibagkar here for comparison.

corresponding to 0, 38, 76 $_2$ (0, 5, 10 and 21% O_2match the target PO and 160 torr respectively) used to bubble the siloxanes in the corresponding tubes.

Figure 4

9.77	0.0010 8 ± 1.16 × $^{-5}$10	0.1105 ± 1.05 × $^{-3}$10	−1.12 ± 6.9 × $^{-5}$10	−9.75 ± 3.9 × $^{-4}$10	0.0015 ± 2.4 × $^{-5}$10	0.1472 ± 1.34 × $^{-3}$10	7 T	HMDSO
11.3	0.0012 5 ±	0.1107 ± 5.04	−1.41 × $^{-6}$10	−1.3 × ± $^{-3}$10	0.0013 ± 1.75	0.1598 ± 8.78	9.4 T	HMDSO

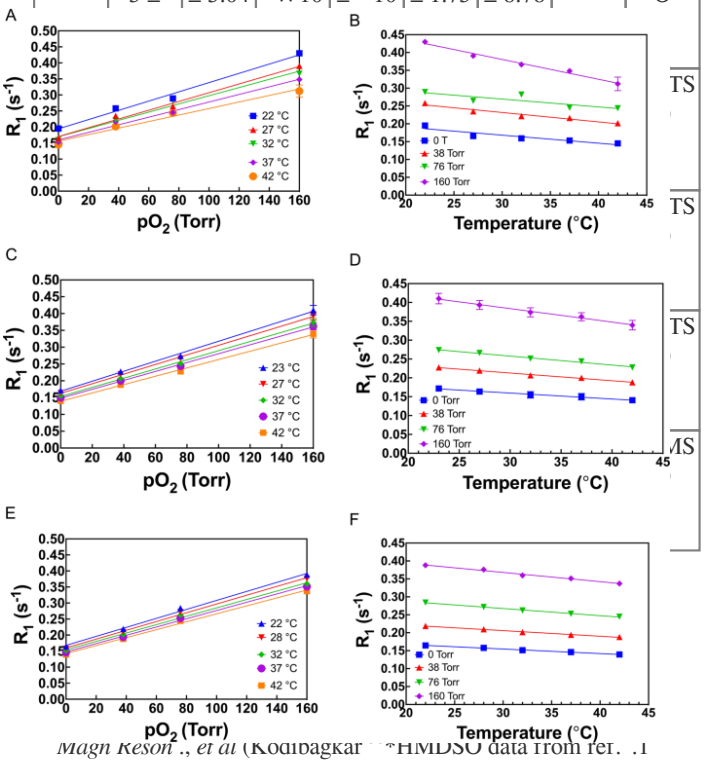

Magn Reson ., et al (Kodibagkar "HMDSO data from ref. .1 , 743–748) reproduced here for comparison.**55** *Med*

Table 2 Summary of temperature dependence of calibration constants of siloxanes measured at different fields.

of OMTSO at 4.7 T $_1$Dependence of spin lattice relaxation rate R) and temperature **E**,**C**,**A** ($_2$) on p**OF**,**E**) and 9.4 T (**D**,**C**), 7 T (**B**,**A**( ).**F**,**D**,**B**(

was determined at 4.7 T $_2$ of OMTSO on pO_1The dependence of R (Fig. 4A,B), 7 T (Fig. 4C,D) and 9.4 T (Fig. 4E,F) and was also observed to be linear at both fields and all temperatures studied. The temperature dependence of constants A′ and B′ was determined by a linear fit of the constants at different temperatures at 4.7 T, 7 T and error for OMTSO $_2$9.4 T (Supplementary Fig. S3A–F). Relative PO ranged between 0.85–1.12 torr/°C in the physiologically relevant range at 9.4 T and was observed to be between 0.65–1.35 torr/°C $_2$PO at 4.7 T and ~ 0.87–1.2 torr/°C at 7 T (Supplementary Fig. S3G). E.g. error was calculated to be ~ 0.7 torr/°C, 0.9 torr/°C and $_2$relative PO 0.88 torr/°C at fields of 4.7 T, 7 T and 9.4 T, respectively, for a was $_2$ of PDMSO on pO_1 of 5 torr. The dependence of R_2PO determined at 7 T (Fig. 5) and was also found to be linear at all

Figure 5

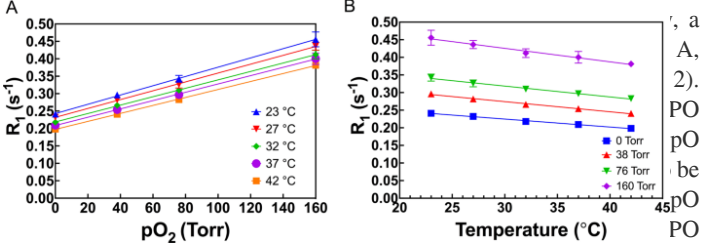

, a A, 2). PO pO be pO PO maps from the calibration data at 7 T and 37 $_2$, we computed PO_2PO °C (using the corresponding constants shown in Table 2) for HMDSO, OMTSO and PDMSO. These are shown in Fig. 6 and

at 7 T was characterized as a function of temperature.

At a given temperature and magnetic field the linear relationship and temperature (defined by Eq. 3) determines the $_2$between PO . The intercept A′ represents the $_2$ to changes in PO$_1$sensitivity of R relaxation rate observed under anoxic condition (the diamagnetic,) and its inverse represents $_{1D}$oxygen independent contribution R displayed by the probe. The slope B′ represents the $_1$maximum T sensitivity of the probe's relaxation rate to the changes in oxygenation) of oxygen to the $_{1p}$and is a ratio of the paramagnetic contribution (R relaxation rate of the probe and the solubility of oxygen in the probe. The ratio η = slope/intercept (B′/A′) is a parameter that helps in determining and comparing the sensitivity index of different MRI reporter molecules. A larger slope B′ and smaller intercept A′ $_2$PO but also indicates $_2$represent greater sensitivity to changes in PO longer imaging times. Since a smaller A′ implies a larger maximum (observed under anoxic or hypoxic conditions which are usually of $_1$T interest in studying pathologies), an adequate sampling of the recovery curves would require the use of longer recovery time TR for imaging. We characterized the relaxation behavior of the linear and cyclic siloxanes by comparing the magnetization recovery curves (Supplementary Fig. S1). $_2$) vs 21% O_2 (0% O_2after bubbling with N behavior was not observed in any of the $_1$Bi-exponential T magnetization recovery curves of the evaluated linear and cyclic siloxanes suggesting that the availability of oxygen to all the protons (e.g end chain vs backbone for linear siloxanes) was unhindered. We observed a decrease in η with respect to an increase in chain length of the linear siloxanes and the η values ranged from 8.2–11.6 × sensitivity. Another $_2$ with only small changes in PO^{-1} torr^{-3}10 important observation was that anoxic relaxation rate (A′) increased with increasing chain length of the siloxanes and was higher for cyclic siloxanes than the linear siloxanes. This is again consistent with and is a [51] and alkanes[50]the observations for perfluoroalkanes consequence of the reduction of molecular tumbling rate for larger chain lengths leading to an increase in relaxation rate. The higher and hence $_1$anoxic relaxation rate indicates a shorter maximum T mapping for the larger siloxanes $_1$potentially less time needed for T which can be further exploited to map tissue oxygenation faster than HMDSO. The B′ value remained similar between the linear and cyclic siloxanes indicating that the solubility of oxygen and its proximity to the methyl protons remains similar between the siloxanes of different chain lengths and structures.

Performing MR oximetry at higher magnetic field strengths has the following advantages: 1) resonances have larger chemical shift separation between them which aids in selective excitation of the siloxane resonance as well as the suppression of the water and fat resonances, 2) increase in net magnetization, leading to improved over the $_1$signal-to-noise, 3) improved dynamic range in T range resulting in more accurate $_2$physiological PO measurements. On the other hand, the relaxation times tend to $_2$pO which might result in an [52,53]increase at higher magnetic fields mapping. Our goal was to $_2$increase in the total imaging time for PO s of HMDSO and OMTSO at 7 T and $_1$evaluate the relationship of T 9.4 T and also help in determining the choice of siloxane for applications requiring higher temporal resolution. Our results suggest = 0 torr and $_2$ was constant at 9 s at PO$_1$that at 37 °C for HMDSO, T = 160 torr on changing the field $_2$ ranged from to 3.5–3.2 s at PO obtained $_1$ strength from 7 T to 9.4 T, which differed by ~ 2% from T determination as $_2$. Also, the calculated relative error in PO[38]at 4.7 T given by Eq. [8] at 37 °C was ~ 0.7 torr/°C at 7 T and ~ 1 torr/°C at value was 5 torr. Since the maximum $_2$9.4 T when the actual PO (and hence potentially imaging time) at 7 T and 9.4 T was same as $_1$T for 4.7 T with no significant increase of temperature-fluctuation determination, PISTOL oximetry using $_2$induced error in PO HMDSO would be improved at higher magnetic field strengths. = 0 torr $_2$ ranged from 6.3–6.8 s at PO$_1$Similarly, for OMTSO the T

) **A** of PDMSO on ($_1$Dependence of spin lattice relaxation rate R) 7 T.**B** and temperature at ($_2$pO

Figure 6

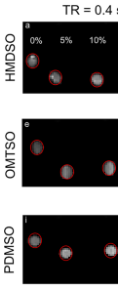

calibration $_2$ maps from the pO$_1$Representative MR images and T) **h–e**), OMTSO (**d–a** maps for HMDSO ($_2$along with predicted pO) at 37 °C and 7 T. In each figure the tubes from left**l–i**and PDMSO ( ), $_2$ (balance $N_2$to right were bubbled with 0%, 5%, 10% and 21% O respectively. All the images were analyzed using MATLAB R2018b (MathWorks, https://www.mathworks.com/products/matlab.html).

Discussion

reporter $_2$HMDSO has been previously characterized as a pO H MR [1]molecule for quantitative oximetry using the PISTOL and HMDSO based nanoemulsions have also [38,39]oximetry technique . [44,45] at 4.7 T*in vitro* and *in vivo*been used to report oxygenation Furthermore, PDMSO nanoemulsions have been used for cell at 7 T. In this [46]labelling and oximetry of neural stem/progenitor cells study we had several goals. Firstly, we aimed to expand the utility of the PISTOL technique for MR oximetry by identifying other reporter molecules. Temperature-dependent $_2$siloxanes for use as PO calibration of HMDSO was conducted at 7 T and 9.4 T to study the effect of magnetic field on calibration of HMDSO and to extend its sensor (at 4.7 T) to higher $_2$previously demonstrated utility as PO fields (7 T and 9.4 T). Based on initial observations at 4.7 T, the reporter OMTSO was further evaluated at higher $_2$promising PO fields (7 T and 9.4 T) and calibration curves were characterized as a function of temperature. Finally, given the prior application of , its calibration curve [46]PDMSO at 7 T for cell labelling and oximetry

siloxanes.

In summary, we have demonstrated for the first time the feasibility H [1]-sensing probes for [2]of various linear and cyclic siloxanes as pO MR oximetry. Of these OMTSO can be identified as a promising probe which could enable faster mapping of tissue oxygenation [2]pO than HMDSO without a significant drop in sensitivity. Alternatively, for applications requiring better temporal resolution or for cell labelling applications, one can use cyclic or long chain linear siloxanes, such as PDMSO, along with a recently developed pulse . In general, all the siloxanes [55]H MR oximetry[1]sequence for faster studied here, with a broad range of boiling points and dynamic range H MR [1]'s, can be used for diversifying the applications of [1]of T oximetry.

Materials and Methods

The linear siloxanes HMDSO, OMTSO, DMTSO, DDMPSO, and cyclic siloxanes OMCTSO and DMCPSO were purchased from Sigma-Aldrich (St Louis, MO). PDMSO (MW = 410, viscosity = 2 cSt) was purchased from Alfa Aeser (Tewksbury, MA). All the materials were used as received and all the experiments were conducted without any dilutions i.e. used 'neat'.

-For the sample preparation, each siloxane (1 ml) was placed in 4 gas tight NMR glass tubes (Wilmad Taperlok, Buena, NJ) and saturated by bubbling for 15 minutes with varying standard of gases including), respectively. Gases with [2] (balance $N_2$0%, 5%, 10%, and 21% O varying oxygen concentrations were made by mixing nitrogen and air in varying proportions in a HypoxyDial (STARR Life Sciences meter was connected in line with the [2]Corp.; Oakmont, PA). A PO output of the HypoxyDial in order to verify the accuracy of the HypoxyDial. The tubes were then sealed. For measurement of the , the temperature of the water pad was [1]temperature dependence of T varied between 17 to 52 °C. A fiber optic probe (FISO Technologies Inc., Quebec, Canada) was used to measure the temperature of the tubes.

MR experiments were performed on a Varian Inova 4.7 T, Bruker BioSpec 7 T and Varian Inova 9.4 T. The tubes were placed together measurements were performed [1]on a pad with circulating water and T after the tube temperature [38,39]using previously described methods was allowed to equilibrate at the desired value for 10–20 mins using a measurement was conducted by [1]surface or volume coil. Briefly, T using pulse-burst saturation recovery with a variable TR ranging from data were fit to a single exponential, 3-parameter [1]0.1–55 ms. T magnetization recovery equation using the Levenberg-Marquardt algorithm. The data at each temperature was then fit into the Eqs. [4–7] described earlier to obtain the corresponding calibration values. MATLAB R2018b (MathWorks, Natick, [1]constants and T maps and [1]MA) was used to analyze the images and compute T maps. Using equation [8], the dependence of errors in [2]pO determination per 1 °C change due to temperature fluctuations [2]PO was simulated for oxygenation levels in relevant hypoxic range (0 torr to 50 torr) at 37 °C.

= 160 torr over the range of magnetic fields [2] and around 2.8 s at pO strengths studied. Thus, the changes in the fields strength will not result in a substantial increase in the imaging time for OMTSO and) are similar to that of HMDSO siliconethe η and relative signal (α (Table 1). Further, the calibration of OMTSO and PDMSO demonstrated that longitudinal relaxation rate of both the siloxanes at temperatures in the [2]varied linearly with respect to changes in PO physiological range, demonstrating the potential of OMTSO and . At a temperature[2]PDMSO to measure dynamic changes in tissue PO of 37 °C OMTSO and PDMSO had an oxygen sensitivity similar to) at all $^{-1}$ torr^{-1}HMDSO (B′ values ranging from 0.0011 to 0.0013 s three fields. It should be also noted that boiling point of OMTSO (153 °C) is higher than the boiling point of HMDSO (101 °C).This suggests that it maybe be more advantageous to use OMTSO for generating nanoemulsions for cell labelling applications than) as it would be less volatile during the [45]HMDSO (used previously determination [2]. The simulated errors in pO[54]emulsification process due to temperature fluctuations for OMTSO as well as PDMSO were found to be in the same range as HMDSO at 4.7 T, 7 T and 9.4 T.

in We have previously demonstrated the feasibility of mapping following intra-tissue injection of 'neat' HMDSO [2] pO*vivo* . Dilution of the [39,44,55]as well as HMDSO based nanoemulsions calibration curve [2]siloxane in a solvent can potentially affect the PO) in a "concentration-dependent" manner by [1] or R_1(and hence T changing the intercept due to changes in the dipole-dipole interactions of the siloxane protons with the solvent protons, although . studied the dependence *et al*this was not tested here. Jamrogiewicz H relaxation times of linear HMDSO on dilution using a mixture [1]of of carbon tetrachloride with deuterated benzene and found that did not significantly depend on the analyte concentration in the [1]T . Dilution of [48]sample or the mutual ratio of the solvents used siloxanes in solvents can also affect the slope of the calibration curve as the oxygen solubility may change based on solvent used and the siloxane concentration. Dilution in tissue by use of less siloxane administered per tissue volume or by diluting a siloxane emulsion is unlikely to affect the calibration as the siloxane is restricted to a local partitioned environment consisting solely of other siloxane molecules and dissolved gasses in either case. We recommend using undiluted mapping applications in order to maintain the highest [2]probes for PO signal to noise ratio.

In general, siloxanes are considered non-toxic or minimally toxic and . However, [47]toxicity decreases with increasing molecular weight use. *in vivo*individual siloxanes should be evaluated for safety before Previous studies have shown that HMDSO is quite inert, and exhibited minimal toxicity in rats tested for subchronic inhalation > 5 ml/kg) was found in rats and [50]. No oral toxicity (LD[56,57]toxicity no irritation and acute toxicity was reported in Draize tests of skin or . In our previous studies, we saw [58]eye irritancy in a study in rabbits no overt signs of toxicity, inflammation or discomfort after injection into muscle, although no [44] or HMDSO nanoemulsions[39]of HMDSO microscopic analyses were performed. Cytotoxicity analysis of HMDSO nanoemulsions showed that the half maximal inhibitory in 3T3 [45]) at a concentration of 0.4–1% (v/v)[50]concentration (IC > 2% (v/v) was reported for PDMSO [50]fibroblast cells while a IC . These [46] nanoemulsions in mouse neural progenitor/stem cells findings indicate that the use of siloxanes, especially longer chain siloxanes may be feasible for human applications. In particular, the use of siloxane emulsions for labelling transplanted cells and monitoring cell health is promising due to the trace amounts used. H MR oximetry in [1]Further, the PISTOL technique used for conjunction with siloxanes utilizes pulse sequence components that are readily available on clinical MRI scanners such as selective RF pulses (for excitation of the siloxane resonance and suppression of fat mapping). This [1]and water signals) and echoplanar readout (for fast T H MR oximetry using [1]adds to the promise of clinical translation of

استنتاج

ref_str

- the lead **Kulkarni, A. C., Kuppusamy, P. & Parinandi, N. Oxygen,** actor in the pathophysiologic drama: enactment of the trinity of normoxia, hypoxia, and hyperoxia in disease and therapy. Antioxid Redox Signal 9, 1717–1730, https://doi.org/10.1089/ars.2007.1724(2007).
- importance in tumor biology, **atum, J. L. et al. Hypoxia:**T noninvasive measurement by imaging, and value of its measurement in the management of cancer therapy. International journal of radiation biology 82, 699–757, https://doi.org/10.1080/09553000601002324(2006).
- Revisiting the essential role of oxygen **Gordillo, G. M. & Sen, C. K.** in wound healing. Am J Surg 186, 259–263 (2003).
- **Ruthenborg, R. J., Ban, J. J., Wazir, A., Takeda, N. & Kim, J. W.** - Regulation of wound healing and fibrosis by hypoxia and hypoxia inducible factor-1. Mol Cells 37, 637–643, https://doi.org/10.14348/molcells.2014.0150(2014).
- The Role of Oxygen **Townley-Tilson, W. H., Pi, X. & Xie, L.** Sensors, Hydroxylases, and HIF in Cardiac Function and Disease. Oxid Med Cell Longev 2015, 676893, https://doi.org/10.1155/2015/676893(2015).
- oxidative stress, hypoxia, and heart failure. J **Giordano, F. J. Oxygen,** Clin Invest 115, 500–508, https://doi.org/10.1172/JCI24408(2005).
- Role of hypoxia in obesity-induced disorders of glucose **Yin, J. et al.** and lipid metabolism in adipose tissue. Am J Physiol Endocrinol Metab 296, E333–342, https://doi.org/10.1152/ajpendo.90760.2008(2009).
- and **Solaini, G., Baracca, A., Lenaz, G. & Sgarbi, G. Hypoxia** mitochondrial oxidative metabolism. Biochim Biophys Acta 1797, 1171 1177, https://doi.org/10.1016/j.bbabio.2010.02.011(2010).
- Regulation **Ban, J. J., Ruthenborg, R. J., Cho, K. W. & Kim, J. W.** of obesity and insulin resistance by hypoxia-inducible factors. Hypoxia (Auckl) 2, 171–183, https://doi.org/10.2147/HP.S68771(2014).
- Hypotension, hypoxia, and head injury: frequency, **Manley, G. et al.** duration, and consequences. Arch Surg 136, 1118–1123 (2001).
- **Carreau, A., El Hafny-Rahbi, B., Matejuk, A., Grillon, C. &** Why is the partial oxygen pressure of human tissues a **Kieda, C.** crucial parameter? Small molecules and hypoxia. J Cell Mol Med 15, 1239–1253, https://doi.org/10.1111/j.1582-4934.2011.01258.x(2011).
- Hypoxia-induced oxidative stress in **Li, S. Y., Fu, Z. J. & Lo, A. C.** ischemic retinopathy. Oxid Med Cell Longev 2012, 426769, https://doi.org/10.1155/2012/426769(2012).
- Lung oxidative damage by **Araneda, O. F. & Tuesta, M.** hypoxia. Oxid Med Cell Longev 2012, 856918, https://doi.org/10.1155/2012/856918(2012).
- **Bhattacharyya, A., Chattopadhyay, R., Mitra, S. & Crowe, S. E.** Oxidative stress: an essential factor in the pathogenesis of gastrointestinal mucosal diseases. Physiol Rev 94, 329–354, https://doi.org/10.1152/physrev.00040.2012(2014).
- -Regulatory systems for hypoxia-**Kim, H. A., Rhim, T. & Lee, M.** nducible gene expression in ischemic heart disease gene therapy. Adv Drug Deliv Rev 63, 678–687, https://doi.org/10.1016/j.addr.2011.01.003(2011).
- Oxidative Stress Related Diseases in **Ozsurekci, Y. & Aykac, K.** Newborns. Oxid Med Cell Longev 2016, 2768365, https://doi.org/10.1155/2016/2768365(2016).
- Hypoxia and **Eales, K. L., Hollinshead, K. E. & Tennant, D. A.** metabolic adaptation of cancer cells. Oncogenesis 5, e190, https://doi.org/10.1038/oncsis.2015.50(2016).
- Oxidative stress, tumor microenvironment,**Fiaschi, T. & Chiarugi, P.** and metabolic reprogramming: a diabolic liaison. Int J Cell Biol 2012, 762825, https://doi.org/10.1155/2012/762825(2012).
- definitions and current **Hockel, M. & Vaupel, P. Tumor hypoxia:** clinical, biologic, and molecular aspects. Journal of the National Cancer Institute 93, 266–276 (2001).
- hypoxia in cancer therapy. Methods **Brown, J. M. Tumor** Enzymol 435, 297–321, https://doi.org/10.1016/S0076-6879(07)35015-5(2007).
- **Shannon, A. M., Bouchier-Hayes, D. J., Condron, C. M. &** chemotherapeutic resistance and **Toomey, D. Tumour hypoxia,** hypoxia-related therapies. Cancer treatment reviews 29, 297–307 (2003).
- Targeting hypoxia in cancer **Wilson, W. R. & Hay, M. P.** therapy. Nature reviews. Cancer 11, 393–410, https://doi.org/10.1038/nrc3064(2011).
- The OxyLite: a fibre-optic oxygen **Griffiths, J. R. & Robinson, S. P.** sensor. Br J Radiol 72, 627–630, https://doi.org/10.1259/bjr.72.859.10624317(1999).
- Near-infrared spectroscopy as an index **Murkin, J. M. & Arango, M.** of brain and tissue oxygenation. Br J Anaesth 103(Suppl 1), i3–13, https://doi.org/10.1093/bja/aep299(2009).
- In vivo oxygen imaging using green fluorescent **Takahashi, E. et al.** protein. Am J Physiol Cell Physiol 291, C781–787, https://doi.org/10.1152/ajpcell.00067.2006(2006).
- Immunohistochemical detection of tumour**Young, R. J. & Moller, A.** hypoxia. Methods Mol Biol 611, 151–159, https://doi.org/10.1007/978-1-60327-345-9_12(2010).
- **Lewis, J. S., McCarthy, D. W., McCarthy, T. J., Fujibayashi, Y. &** Evaluation of 64Cu-ATSM in vitro and in vivo in a **Welch, M. J.** hypoxic tumor model. J Nucl Med 40, 177–183 (1999).
- -High sensitivity lanthanide (III) based probes for MR-**Aime, S. et al.** edical imaging. Coordin. Chem Rev 250, 1562–1579, https://doi.org/10.1016/j.ccr.2006.03.015(2006).
- Pimonidazole: a novel hypoxia marker for **Varia, M. A. et al.** complementary study of tumor hypoxia and cell proliferation in cervical carcinoma. Gynecol Oncol 71, 270–277, https://doi.org/10.1006/gyno.1998.5163(1998).
- Detection of hypoxia in human squamous cell **Evans, S. M. et al.** carcinoma by EF5 binding. Cancer Res 60, 2018–2024 (2000).
- In vivo study of **Tamura, M., Hazeki, O., Nioka, S. & Chance, B.** tissue oxygen metabolism using optical and nuclear magnetic resonance spectroscopies. Annu Rev Physiol 51, 813–834, https://doi.org/10.1146/annurev.ph.51.030189.004121(1989).
- How does blood oxygen level-dependent **Baudelet, C. & Gallez, B.** (BOLD) contrast correlate with oxygen partial pressure (pO2) inside tumors? Magn Reson Med 48, 980–986, https://doi.org/10.1002/mrm.10318(2002).
- -Simultaneous measurement of tissue oxygen level-**Ding, Y. et al.** ependent (TOLD) and blood oxygenation level-dependent (BOLD) effects in abdominal tissue oxygenation level studies. J Magn Reson Imaging 38, 1230–1236, https://doi.org/10.1002/jmri.24006(2013).
- Oxygen-Enhanced MRI Accurately Identifies, **O'Connor, J. P. et al.** Quantifies, and Maps Tumor Hypoxia in Preclinical Cancer Models. Cancer Res 76, 787–795, https://doi.org/10.1158/0008-5472.CAN-15-2062(2016).
- GdDO3NI, a nitroimidazole-based T1 MRI **Gulaka, P. K. et al.** contrast agent for imaging tumor hypoxia in vivo. Journal of biological inorganic chemistry: JBIC: a publication of the Society of Biological Inorganic Chemistry 19, 271–279, https://doi.org/10.1007/s00775-013-1058-5(2014).
- instrumentation, and **Ahmad, R. & Kuppusamy, P. Theory,** applications of electron paramagnetic resonance oximetry. Chem Rev 110, 3212–3236, https://doi.org/10.1021/cr900396q(2010).
- **Mason, R. P., Rodbumrung, W. & Antich, P. P.** : a sensitive 19F NMR indicator of tumor **Hexafluorobenzene** oxygenation. NMR Biomed 9, 125–134 (1996).
- Novel **Kodibagkar, V. D., Cui, W., Merritt, M. E. & Mason, R. P.** 1H NMR approach to quantitative tissue oximetry using

hexamethyldisiloxane. Magn Reson Med 55, 743–748, https://doi.org/10.1002/mrm.20826(2006).

- **Kodibagkar, V. D., Wang, X., Pacheco-Torres, J., Gulaka, P. & Mason, R. P.** Proton imaging of siloxanes to map tissue oxygenation levels (PISTOL): a tool for quantitative tissue oximetry. NMR Biomed 21, 899–907, https://doi.org/10.1002/nbm.1279(2008).
- **Swartz, H. M. et al.** Advances in probes and methods for clinical EPR oximetry. Adv Exp Med Biol 812, 73–79, https://doi.org/10.1007/978-1-4939-0620-8_10(2014).
- **Dardzinski, B. J. & Sotak, C. H.** Rapid tissue oxygen tension mapping using 19F inversion-recovery echo-planar imaging of perfluoro-15-crown-5-ether. Magn Reson Med 32, 88–97 (1994).
- **Bourke, V. A. et al.** Correlation of radiation response with tumor oxygenation in the Dunning prostate R3327-AT1 tumor. Int J Radiat Oncol Biol Phys 67, 1179–1186, https://doi.org/10.1016/j.ijrobp.2006.11.037(2007).
- **Zhao, D., Constantinescu, A., Chang, C. H., Hahn, E. W. & Mason, R. P.** Correlation of tumor oxygen dynamics with radiation response of the dunning prostate R3327-HI tumor. Radiat Res 159, 621–631 (2003).
- **Gulaka, P. K. et al.** Hexamethyldisiloxane-based nanoprobes for (1) H MRI oximetry. NMR Biomed 24, 1226–1234, https://doi.org/10.1002/nbm.1678(2011).
- **Menon, J. U. et al.** Dual-modality, dual-functional nanoprobes for cellular and molecular imaging. Theranostics 2, 1199–1207, https://doi.org/10.7150/thno.4812(2012).
- **Addington, C. P. et al.** Siloxane Nanoprobes for Labeling and Dual Modality Functional Imaging of Neural Stem Cells. Annals of biomedical engineering 44, 816–827, https://doi.org/10.1007/s10439-015-1514-1(2016).
- **Mojsiewicz-Pienkowska, K., Jamrogiewicz, M., Szymkowska, K. & Krenczkowska, D.** Direct Human Contact with Siloxanes (Silicones) - Safety or Risk Part 1. Characteristics of Siloxanes (Silicones). Front Pharmacol 7 (132), https://doi.org/10.3389/Fphar.2016.00132(2016).
- **Jamrogiewicz, Z., Mojsiewicz-Pienkowska, K., Jachowska, D. & Lukasiak, J.** Study on the dependence of longitudinal relaxation time in H-1 NMR method on the structure of polydimethylsiloxanes and optimization of spectra registration parameters. Polimery-W 50, 737–741, https://doi.org/10.14314/polimery.2005.737(2005).
- **Kodibagkar, V. D., Wang, X. & Mason, R. P.** Physical principles of quantitative nuclear magnetic resonance oximetry. Front Biosci 13, 1371–1384, doi:2768 [pii] (2008).
- **Hamza, M. A., Serratrice, G., Stebe, M. J. & Delpuech, J. J.** Fluorocarbons as Oxygen Carriers.2. An Nmr-Study of Partially or Totally Fluorinated Alkanes and Alkenes. J Magn Reson 42, 227–241 (1981).
- **Woessner, D. E.** Proton Spin-Lattice Relaxation of N-Paraffins in Solution. J Chem Phys 41, 84-&, https://doi.org/10.1063/1.1725655(1964).
- **Korb, J. P. & Bryant, R. G.** Magnetic field dependence of proton spin-lattice relaxation times. Magn Reson Med 48, 21–26, https://doi.org/10.1002/mrm.10185(2002).
- **Bottomley, P. A., Foster, T. H., Argersinger, R. E. & Pfeifer, L.** A review of normal tissue hydrogen NMR relaxation times and **M.** relaxation mechanisms from 1-100 MHz: dependence on tissue type, NMR frequency, temperature, species, excision, and age. Med Phys 11, 425–448, https://doi.org/10.1118/1.595535(1984).
- **Sharma, S. K., Lowe, K. C. & Davis, S. S.** Emulsification Methods for Perfluorochemicals. Drug Development and Industrial Pharmacy 14, 2371–2376 (1988).
- **Vidya Shankar, R. & Kodibagkar, V. D.** A faster PISTOL for (1) H MR-based quantitative tissue oximetry. NMR Biomed 32, e4076, https://doi.org/10.1002/nbm.4076(2019).
- **Cassidy, S. L. et al.** Hexamethyldisiloxane: A 13-week subchronic whole-body vapor inhalation toxicity study in Fischer 344 rats. Int J Toxicol 20, 391–399, https://doi.org/10.1080/10915810175333367(2001).
- **Dobrev, I. D. et al.** Closed-chamber inhalation pharmacokinetic studies with hexamethyldisiloxane in the rat. Inhal Toxicol 15, 589–617, https://doi.org/10.1080/08958370390205083(2003).
- **Parent, R. A.** Acute Toxicity Data Submissions. Int J Toxicol 19, 331–373 (2000).

IJSURP Publishing Academy

International Journal Of Scientific And University Research Publication

Multi-Subject Journal

Editor.

International Journal Of Scientific And University Research Publication

+965 99549511

+90 5374545296

+961 03236496

+44 (0)203 197 6676

www.ijsurp.com